BNUT

Iranica Journal of Energy & Environment
Journal Homepage: www.ijee.net
IJEE an official peer review journal of Babol Noshirvani University of Technology, ISSN:2079-2115

# Analysis of Formability in Stamping of Metallic Bipolar Plates with Parallel Flow Field for Proton Exchange Membrane Fuel Cells using Adaptive Neuro-fuzzy Inference System

V. Modanloo*, A. Mashayekhi, B. Akhoundi

*Department of Mechanical Engineering, Sirjan University of Technology, Sirjan, Iran*

*PAPER INFO*

*Paper history:*
Received 06 August 2023
Accepted in revised form 09 September 2023

*Keywords*:
Adaptive neuro-fuzzy inference system
Bipolar plate
Proton exchange membrane fuel cell
Thickness reduction
Titanium sheet

*ABSTRACT*

Bipolar plates (BPPs) play an important role in PEM fuel cells in terms of weight and cost points of view. In this paper, the manufacturing of titanium BPPs with parallel flow field was experimentally and numerically studied. In this regard, a stamping die with a parallel pattern is conducted to perform the experiments. Then, the process was modeled via the finite element (FE) simulation. By comparing simulation and experiment results, it was found that the results are in good agreement and hereupon, the accuracy of the FE model was verified. To evaluate the sheet formability, a set of FE experiments was designed through the response surface methodology (RSM). The die clearance, forming velocity, and friction coefficient were considered input parameters, and the maximum thickness reduction (MTR) of the sheet was assumed to be the output. The results revealed that a lower friction coefficient causes an increase in thickness reduction and finally tearing in the formed BPPs. Moreover, changing the forming velocity has no remarkable influence on the MTR. Afterward, an Adaptive Neuro-Fuzzy Inference System (ANFIS) was trained for predicting the output of the MTR with the three mentioned inputs.

***doi**: 10.5829/ijee.2024.15.02.06*

**NOMENCLATURE**

| | | | |
|---|---|---|---|
| $C$ | Die clearance (mm) | $t_0$ | Initial thickness of the sheet |
| $V$ | Forming velocity (mm/min) | $t_f$ | Final thickness of the formed plate |
| $\mu$ | Friction coefficient | | |

## INTRODUCTION

Over recent years, the proton exchange membrane fuel cell (PEMFC) is considered as an appropriate electrical power source compared with internal combustion engines due to its high efficiency, low working temperature, system durability, and low emission [1]. Figure 1 shows the performance of a PEMFC [2]. As is shown, oxidation reaction is carried out on the channels in the anode side of bipolar plates (BPPs) and hydrogen is decomposed into electrons and positive ions. The electron from decomposition enters the external circuit and then enters to the cathode. The positive ion also goes to the cathode by passing through the electrolyte and turns into water with the oxygen of the air and the electron that entered the cathode from the external circuit. The produced water also exits from the flow path channels on the cathode side of the (BPPs).

The PEMFC has not been commercialized widely due to its higher cost than an internal combustion engine [2]. BPPs are the most important components of a fuel cell since they comprise almost 75 and 45% of its weight and

*Corresponding Author Email: *v.modanloo@sirjantech.ac.ir* (V. Modanloo)

Please cite this article as: V. Modanloo, A. Mashayekhi, B. Akhoundi, 2024. Analysis of Formability in Stamping of Metallic Bipolar Plates with Parallel Flow Field for Proton Exchange Membrane Fuel Cells using Adaptive Neuro-fuzzy Inference System, Iranica Journal of Energy and Environment, 15(2), pp. 170-176. Doi: 10.5829/ijee.2024.15.02.06

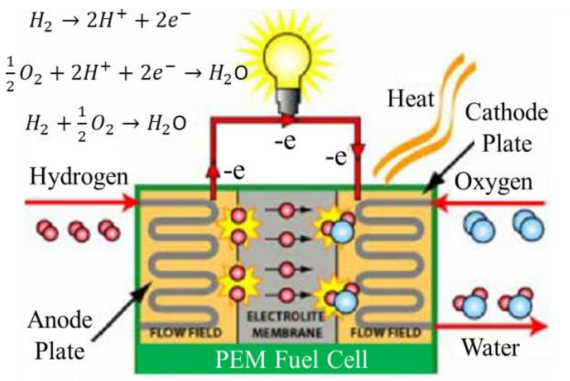


**Figure 1.** A PEMFC with its performance [2]

price, respectively [3]. Various types of materials for the BPP are used in a PEMFC such as graphite [4], polymer [5], and metal [6]. Among the mentioned materials, the metallic BPP has received more attention from researchers due to its supreme physical properties and ease of production [7–9]. In the past two decades, different approaches have been suggested by researchers for fabricating the metallic BPPs including hydroforming [10], gas blow forming [11], rubber pad forming [12], and stamping [13]. Among the mentioned processes, the stamping process exhibits high potential for mass production [14]. Koo et al. [15] studied the influence of variation of the stamping force on the forming behavior of the SS304 thin sheet. They estimated the formability of the microchannels with various punch load and die roundness by applying a dynamic load. They reported that forming depth is enhanced by 7% via a dynamic stamping using a square wave. In addition, thinning is enhanced almost 28% via the stamping process using a sine wave. Hu et al. [16] investigated the stamping of the SS304 sheet by experiment and numerical simulation. They used forming limit diagrams for predicting the forming defects. They stated that wrinkling phenomenon takes place when a lower velocity is used. On the other hand, the crack occurs in the sheet at a higher velocity. Also, a smaller punch radius leads to dramatically thinning. Kim et al. [17] compared the formability of the SS316L BPPs in stamping process by static and dynamic forces. The formability of the stamped BPPs was examined from various points of view (force type, size of force, die radius, and the cycle number). The BPP manufactured using sine wave dynamic load equal to 50 to120 kN, 17 cycles, and 0.3 mm die radius exhibited more channel height (15%) compared with the BPP stamped with a 120 kN static force. The influence of the process parameters on the surface roughness and corrosion resistance of the SS304 stamped BPPs was studied by Dundar et al. [18]. They reported a lower stamping speed, lower surface quality. Furthermore, by decreasing stamping velocity, the corrosion resistance decreases. Accordingly, it is suggested to set a higher stamping velocity for manufacturing BPPs. Chen and Ye [19] used an elastic-plastic deformation FE model by using an updated Lagrangian formulation and scale factor for simulating the micro-stamping process of the SS304 BPPs. They concluded that the results of the improved material model were near to the results of experiment. Smith et al. [20] performed a comparative research to select the most suitable alternative for manufacturing the BPPs. They used materials namely SS316L, high-temperature ferritic SS, AA5086-O, AA1100-O, and commercially pure titanium. The maximum channel height and springback of the stamped plates were considered criteria. Their results demonstrated that the SS316L is the best material for fabricating the BPPs.

ANFIS is a machine learning algorithm that is a powerful combination of neural network and fuzzy logic, to predict outputs based on its inputs. It uses neural network to train the fuzzy parameters of if-then rules inside its fuzzy. Result is a hybrid system capable of training and predicting both numerical and linguistic data, with wide applications introduced by Sobhani et al. [21] and Zhou et al. [22]. Since neural network has lots of applications reported in the literature [23–25], and also fuzzy logic is used in wide range of applications introduced by Benbouhenni [26], Deb et al. [27] and Maraki et al. [28], then a wide range of application can also be imagining for the ANFIS.

Despite valuable research works on manufacturing the metallic BPPs, a study related to the influence of the process parameters on the formability of the titanium sheet (an initial thickness of 0.1 mm) in terms of thickness reduction using the stamping process was not reported based on the best knowledge of the authors. Titanium is a worthy candidate for fabricating metallic BPPs due to its low density and superior corrosion resistance. On the other hand, its formability is poor due to HCP crystal structure. In this research, the influence of the die clearance, forming velocity and coefficient of friction on the MTR of the titanium BPPs is investigated via the RSM method. A verified FE model (with experimental results) was used to carry out the stamping tests designed by the RSM. Also, an ANFIS model was used to predict the MTR.

## FE SIMULATION

In this paper, the ABAQUS software was used to simulate the stamping process to fabricate BPPs for PEM fuel cell. The titanium sheet was modeled deformable and the punch and die were modeled analytical rigid. A CPS4R element (four-node bilinear plane stress) was used for the sheet. Also, the punch and die were not meshed due to analytical rigid considering. To obtain the material properties and then to introduce to the software, tensile test was conducted according to ASTM-E8M standard that prepared specimens are shown in Figure 2. The

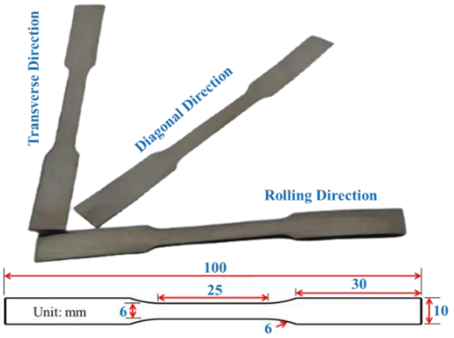


**Figure 2.** Tensile test specimens

**Figure 5.** The used microscope to observe the formed plates and measure their thickness reduction

plastic strain ratio in different directions i.e. rolling, diagonal, and transverse were measured to take into account the anisotropy behavior of the titanium sheet. Figure 3 depicts the 2D FE model with channel dimensions.

## EXPERIMENT

A titanium sheet with a thickness of 0.1 mm was used for manufacturing the metallic BPPs. A 200 kN press machine was applied to carry out the stamping experiments. The used core dies were fabricated with a parallel design and were mounted on the upper and lower dies as is depicted in Figure 4.

To measure the thickness reduction of the stamped samples, first they were cut. Then, they were mounted and polished to be accurately observed throgh an optical (40x) microscope as is shown in Figure 5.

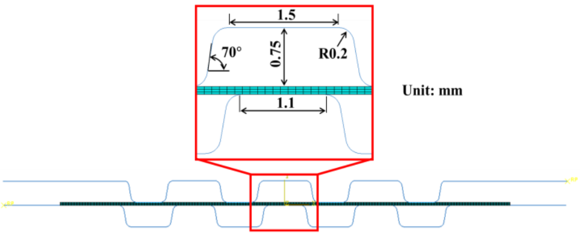


**Figure 3.** 2D FE model with channel dimensions

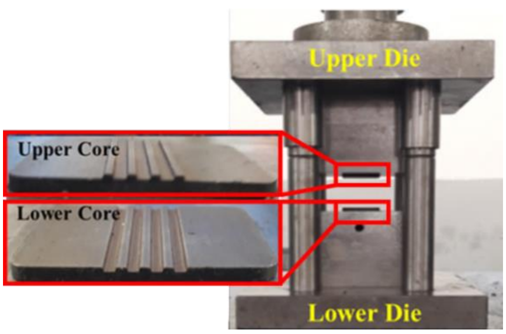


**Figure 4.** The core dies on the upper and lower dies

## RESPONSE SURFACE METHODOLOGY (RSM)

In this paper, the RSM was applied to examine the influence of the input parameters on the maximum thickness reduction of the formed BPPs. In this method, a quadratic full equation expresses the regression model. The goodness (efficiency) of the obtained model can be evaluated using Equation (1) with respect to the results of the ANOVA (analysis of variance) [29] {Modanloo, 2016 #33}. In this equation, $SS_r$ denots the residual and $SS_t$ denotes the total sum of squares [30].

$$R^2 = 1 - \frac{SS_r}{SS_t} \qquad (1)$$

To create the RSM design, stamping parameters including die clearance (*C*), forming velocity (*V*), and coefficient of friction ($\mu$) were considered input parameters. Also, the MTR of the formed BPPs was considered output. Eventually, 20 experiments were considered via the Minitab software [31] as given in Table 1, and then were performed via FE simulation.

## RESULTS AND DISCUSSION

To validate the results of simulation, the thickness of the formed plates was compared with the results of experiment as is presented in Figure 6. As is shown, there is a well agreement between the results. Therefore, the validated FE model was used to perform the designed tests by the RSM. In this paper, Equation (2) was used to calculate MTR [32], in which $t_0$ and $t_f$ indicate initial thickness of the sheet and the final thickness of the stamped BPP, respectively.

$$Thickness\ Reduction\ (\%) = \frac{t_0 - t_f}{t_0} \times 100 \qquad (2)$$

Table 2 presents the results of MTR for all FE experiments. After extracting the results, the ANOVA was carried out for MTR and the model efficiency ($R^2$) was achieved equal to 45.50%. Therefore, the assumption of data normality is not sensible, hence ANOVA cannot be utilized to evaluate the main influence of parameters

**Table 1.** The RSM design

| Run no. | C (mm) | V (mm/min) | μ |
|---|---|---|---|
| 1 | 0.175 | 2 | 0.15 |
| 2 | 0.175 | 2 | 0.15 |
| 3 | 0.15 | 3.5 | 0.1 |
| 4 | 0.175 | 2 | 0.2 |
| 5 | 0.175 | 2 | 0.1 |
| 6 | 0.2 | 2 | 0.15 |
| 7 | 0.175 | 2 | 0.15 |
| 8 | 0.2 | 0.5 | 0.2 |
| 9 | 0.2 | 0.5 | 0.1 |
| 10 | 0.2 | 3.5 | 0.2 |
| 11 | 0.175 | 0.5 | 0.15 |
| 12 | 0.15 | 3.5 | 0.2 |
| 13 | 0.175 | 2 | 0.15 |
| 14 | 0.175 | 2 | 0.15 |
| 15 | 0.15 | 0.5 | 0.1 |
| 16 | 0.175 | 3.5 | 0.15 |
| 17 | 0.15 | 2 | 0.15 |
| 18 | 0.2 | 3.5 | 0.1 |
| 19 | 0.15 | 0.5 | 0.2 |
| 20 | 0.175 | 2 | 0.15 |

**Table 2.** The obtained MTR for designed experiments

| Run no. | MTR (%) |
|---|---|
| 1 | 3.43 |
| 2 | 3.43 |
| 3 | 5.15 |
| 4 | 5.16 |
| 5 | 4.74 |
| 6 | 4.74 |
| 7 | 3.43 |
| 8 | 4.72 |
| 9 | 4.70 |
| 10 | 4.35 |
| 11 | 5.01 |
| 12 | 4.43 |
| 13 | 3.43 |
| 14 | 3.43 |
| 15 | 5.19 |
| 16 | 4.92 |
| 17 | 4.91 |
| 18 | 4.69 |
| 19 | 4.28 |
| 20 | 3.43 |

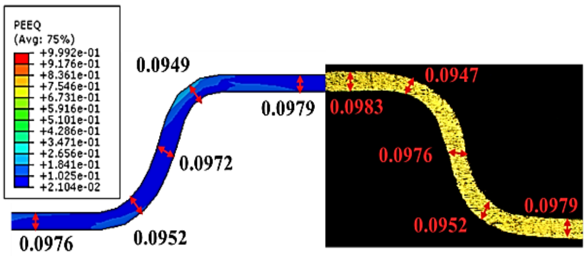


**Figure 6.** Comparison of the numerical and experimental results

and to explore the regression model. Contour plots of input parameters regarding MTR were used to obtain the optimal range of them as shown in Figure 7. The bright blue zone implies how to gain a lower thickness reduction. As is depicted, when all parameters are in their middle value, the desired (minimum) value of the MTR is accessible. However, the experimental investigation proved this fact that lower die clearance and friction condition cause increasing thickness reduction and finally tearing in the formed sample. Figure 8 illustrates a typical rupture at the corner radius zone of the manufactured BPP. In addition, Also, forming velocity does not significantly impact the MTR.

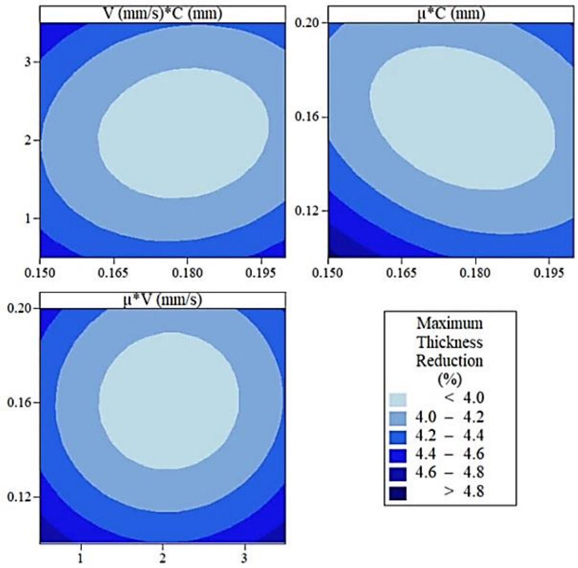


**Figure 7.** Contour plots for the MTR versus input parameters

## ANFIS Model

In this section, an ANFIS model is trained with three inputs of die clearance, forming velocity, and friction coefficient to predict the output of MTR. For this purpose, an ANFIS consisting of 5 layers, is used as shown in Figure 9. Three mentioned inputs go to the first layer, and convert to fuzzy if-then rules using some membership functions. Power of the rules is calculated in the second layer (rule layer), to compute the output signal by multiplying the signals some fuzzy operators. The third layer, node power is calculated and normalizes for each neuron, by diving each power by sum of powers. Fuzzy quantities are de-fuzzyfied in the fourth layer, then the output is calculated in the fifth layer based on sum of incoming signals from the fourth layer.

An ANFIS model with three Gaussian membership functions for each input,78 nodes, 27 linear parameters, 18 nonlinear parameters, 20 training data point, and 27 rules is used for training and prediction. After 10 epochs of training, the ANFIS is well adapted for predicting the maximum thickness, as shown in Figure 10. While the surfaces relating the inputs to the output are shown in Figures 11 and 12, respectively.


**Figure 8.** The ruptured titanium BPP

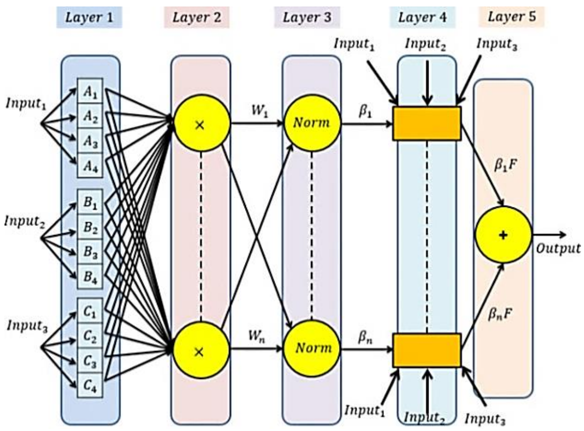


**Figure 9.** Structure of ANFIS- 5 different layers

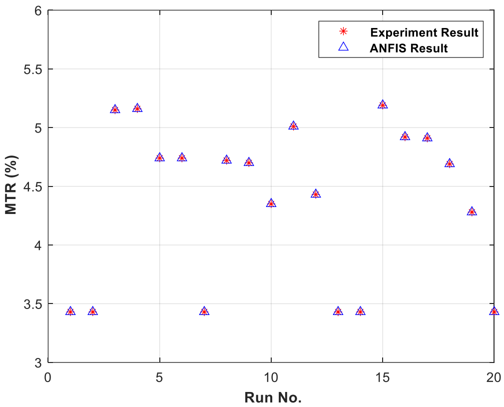


**Figure 10.** Comparing the MTR of the experiments and ANFIS prediction

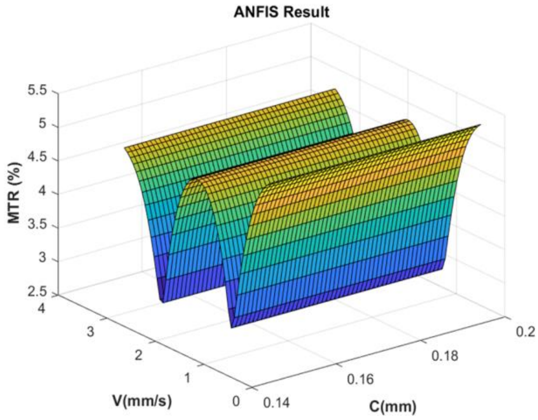


**Figure 11.** ANFIS surface of die clearance (C), forming velocity (V) and the MTR

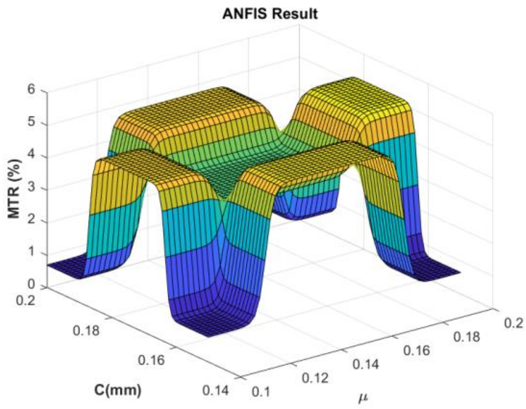


**Figure 12.** ANFIS surface of friction coefficient (μ), die clearance (C), and the MTR.

## CONCLUSION

In this paper, manufacturing of titanium BPPs with parallel flow field via stamping process for PEM fuel cells was studied numerically and experimentally. The influence of stamping process parameters including die clearance, forming velocity, and coefficient of friction on the MTR of the titanium bipolar plats was investigated.

The required tests were designed using the response surface method and were carried out via an experimentally validated FE model. Results demonstrated that increasing friction coefficient results an increased in MTR. Also, the forming velocity is not an effective parameter on the MTR. In addition, an ANFIS model is trained for predicting the MTR, as a function of die clearance, forming velocity, and friction coefficient. Results showed that this method can predict the desired output with an excellent accuracy, due to using a combination of neural network and fuzzy.

## CONFLICT OF INTEREST

The authors declared no potential conflicts of interest.

## REFERENCES


1. Talebi-Ghadikolaee, H., Barzegari, M.M., and Seddighi, S., 2023. Investigation of deformation mechanics and forming limit of thin-walled metallic bipolar plates. *International Journal of Hydrogen Energy*, 48(11), pp.4469–4491. Doi: 10.1016/j.ijhydene.2022.10.270
2. Modanloo, V., Alimirzaloo, V., and Elyasi, M., 2020. Investigation on forming of titanium bipolar plates using micro-stamping process. *International Journal of Engineering*, 33(2), pp.344–349. Doi: 10.5829/ije.2020.33.02b.20
3. Talebi Ghadikolaee, H., Seddighi, S., and Barzegari, M.M., 2023. Study of the forming process effects on the wrinkling and thinning percentage of the micro-channels with serpentine layout. *Hydrogen, Fuel Cell & Energy Storage*, 10(1), pp.81–93. Doi: 10.22104/ijhfc.2023.6007.1255
4. Khatir, F.A., Barzegari, M.M., Talebi-Ghadikolaee, H., and Seddighi, S., 2021. Integration of design of experiment and finite element method for the study of geometrical parameters in metallic bipolar plates for PEMFCs. *International Journal of Hydrogen Energy*, 46(79), pp.39469–39482. Doi: 10.1016/j.ijhydene.2021.09.161
5. Hamilton, P.J., and Pollet, B.G., 2010. Polymer Electrolyte Membrane Fuel Cell (PEMFC) Flow Field Plate: Design, Materials and Characterisation. *Fuel Cells*, 10(4), pp.489–509. Doi: 10.1002/fuce.201000033
6. Barzegari, M.M., and Khatir, F.A., 2019. Study of thickness distribution and dimensional accuracy of stamped metallic bipolar plates. *International Journal of Hydrogen Energy*, 44(59), pp.31360–31371. Doi: 10.1016/j.ijhydene.2019.09.225
7. Elyasi, M., Ghadikolaee, H.T., and Hosseinzadeh, M., 2018. Investigation of dimensional accuracy in forming of metallic bipolar plates with serpentine flow field. *The International Journal of Advanced Manufacturing Technology*, 96(1–4), pp.1045–1060. Doi: 10.1007/s00170-018-1650-5
8. Modanloo, V., Alimirzaloo, V., and Elyasi, M., 2020. Manufacturing of Titanium Bipolar Plates Using Warm Stamping Process. *Arabian Journal for Science and Engineering*, 45(11), pp.9661–9667. Doi: 10.1007/s13369-020-04870-3
9. Modanloo, V., Talebi-Ghadikolaee, H., Alimirzaloo, V., and Elyasi, M., 2021. Fracture prediction in the stamping of titanium bipolar plate for PEM fuel cells. *International Journal of Hydrogen Energy*, 46(7), pp.5729–5739. Doi: 10.1016/j.ijhydene.2020.11.088
10. Mohammadtabar, N., Bakhshi-Jooybari, M., Hosseinipour, S.J., and Gorji, A.H., 2016. Feasibility study of a double-step hydroforming process for fabrication of fuel cell bipolar plates with slotted interdigitated serpentine flow field. *The International Journal of Advanced Manufacturing Technology*, 85(1–4), pp.765–777. Doi: 10.1007/s00170-015-7960-y
11. Moradian, M., Doniavi, A., Modanloo, V., and Alimirzaloo, V., 2017. Process parameters optimization in gas blow forming of pin-type metal bipolar plates using Taguchi and finite element methods. *International Journal of Advanced Design & Manufacturing Technology*, 10(2), pp.101–108.
12. Elyasi, M., Khatir, F.A., and Hosseinzadeh, M., 2017. Manufacturing metallic bipolar plate fuel cells through rubber pad forming process. *The International Journal of Advanced Manufacturing Technology*, 89(9–12), pp.3257–3269. Doi: 10.1007/s00170-016-9297-6
13. Khatir, F.A., Elyasi, M., Ghadikolaee, H.T., and Hosseinzadeh, M., 2017. Evaluation of Effective Parameters on Stamping of Metallic Bipolar Plates. *Procedia Engineering*, 183, pp.322–329. Doi: 10.1016/j.proeng.2017.04.047
14. Modanloo, V., Alimirzaloo, V., and Elyasi, M., 2019. Multi-objective optimization of the stamping of titanium bipolar plates for fuel cell. *ADMT Journal*, 12(4), pp.1–8.
15. Koo, J.-Y., Jeon, Y.-P., and Kang, C.-G., 2013. Effect of stamping load variation on deformation behaviour of stainless steel thin plate with microchannel. *Proceedings of the Institution of Mechanical Engineers, Part B: Journal of Engineering Manufacture*, 227(8), pp.1121–1128. Doi: 10.1177/0954405412462673
16. Hu, Q., Zhang, D., Fu, H., and Huang, K., 2014. Investigation of stamping process of metallic bipolar plates in PEM fuel cell—Numerical simulation and experiments. *International Journal of Hydrogen Energy*, 39(25), pp.13770–13776. Doi: 10.1016/j.ijhydene.2014.01.201
17. Kim, M.-J., Jin, C.-K., and Kang, C.G., 2014. Comparison of formabilities of stainless steel 316L bipolar plates using static and dynamic load stamping. *The International Journal of Advanced Manufacturing Technology*, 75(5–8), pp.651–657. Doi: 10.1007/s00170-014-5986-1
18. Dundar, F., Dur, E., Mahabunphachai, S., and Koç, M., 2010. Corrosion resistance characteristics of stamped and hydroformed proton exchange membrane fuel cell metallic bipolar plates. *Journal of Power Sources*, 195(11), pp.3546–3552. Doi: 10.1016/j.jpowsour.2009.12.040
19. Chen, T.-C., and Ye, J.-M., 2013. Fabrication of micro-channel arrays on thin stainless steel sheets for proton exchange membrane fuel cells using micro-stamping technology. *The International Journal of Advanced Manufacturing Technology*, 64(9–12), pp.1365–1372. Doi: 10.1007/s00170-012-4107-2
20. Smith, T.L., Santamaria, A.D., Park, J.W., and Yamazaki, K., 2014. Alloy Selection and Die Design for Stamped Proton Exchange Membrane Fuel Cell (PEMFC) Bipolar Plates. *Procedia CIRP*, 14, pp.275–280. Doi: 10.1016/j.procir.2014.03.078
21. Sobhani, B., Safarian Zengir, V., and Kianian, M.K., 2019. Modeling, monitoring and prediction of drought in Iran. *Iranian (Iranica) Journal of Energy & Environment*, 10(3), pp.216–224. Doi: 10.5829/ijee.2019.10.03.09
22. Zhou, J., Li, C., Arslan, C.A., Hasanipanah, M., and Bakhshandeh Amnieh, H., 2021. Performance evaluation of hybrid FFA-ANFIS and GA-ANFIS models to predict particle size distribution of a muck-pile after blasting. *Engineering with Computers*, 37(1), pp.265–274. Doi: 10.1007/s00366-019-00822-0
23. Ataee, A., Kazemitabar, J., and Najafi, M., 2020. A Framework for Dry Waste Detection Based on a Deep Convolutional Neural Network. *Iranian (Iranica) Journal of Energy & Environment*, 11(4), pp.248–252. Doi: 10.5829/IJEE.2020.11.04.01

24. Dorrani, Z., Farsi, H., and Mohamadzadeh, S., 2023. Shadow Removal in Vehicle Detection Using ResUNet-a. *Iranian (Iranica) Journal of Energy & Environment*, 14(1), pp.87–95. Doi: 10.5829/IJEE.2023.14.01.11

25. Farhadi, R., Hadavifar, M., Moeinaddini, M., and Amintoosi, M., 2022. Prediction of CO and PM10 in Cold and Warm Seasons and Survey of the Effect of Instability Indices on Contaminants Using Artificial Neural Network: A Case Study in Tehran City. *Iranian (Iranica) Journal of Energy & Environment*, 13(1), pp.71–78. Doi: 10.5829/IJEE.2022.13.01.08

26. Benbouhenni, H., 2021. A Novel Direct Active and Reactive Power Control Method Using Fuzzy Super Twisting Algorithms and Modified Space Vector Modulation Technique for an Asynchronous Generator-based Dual-rotor Wind Powers. *Iranian (Iranica) Journal of Energy & Environment*, 12(2), pp.109–117. Doi: 10.5829/ijee.2021.12.02.02

27. Deb, N., Alam, M.Z., Rahman, T., Jami, M.S., Bt Mansor, M.F., and Tajuddin, H.B.A., 2023. Design and Analysis of a Fuel Cell and Batteries in Energy Production for Electric Vehicle. *Iranian (Iranica) Journal of Energy & Environment*, 14(3), pp.301–313. Doi: 10.5829/ijee.2023.14.03.11

28. Maraki, M.R., Tagimalek, H., and Pasoodeh, B., 2022. Provide a Modeling Algorithm for Mechanical Properties of Friction Stir Welding of 5 Series Aluminum and Pure-Copper Based on Fuzzy Logic. *Iranian (Iranica) Journal of Energy & Environment*, 13(2), pp.169–175. Doi: 10.5829/IJEE.2022.13.02.08

29. Modanloo, V., and Alimirzaloo, V., 2016. Minimization of the sheet thinning in hydraulic deep drawing process using response surface methodology and finite element method. *International Journal of Engineering*, 29(2), pp.264–273. Doi: 10.5829/idosi.ije.2016.29.02b.16

30. Hasan Nejad, S.J., Hasanzadeh, R., Doniavi, A., and Modanloo, V., 2017. Finite element simulation analysis of laminated sheets in deep drawing process using response surface method. *The International Journal of Advanced Manufacturing Technology*, 93(9–12), pp.3245–3259. Doi: 10.1007/s00170-017-0780-5

31. Modanloo, V., Doniavi, A., and Hasanzadeh, R., 2016. Application of multi criteria decision making methods to select sheet hydroforming process parameters. *Decision Science Letters*, 5(3), pp.349–360. Doi: 10.5267/j.dsl.2016.2.005

32. Modanloo, V., Gorji, A., and Bakhshi-Jooybari, M., 2019. A Comprehensive Thinning Analysis for Hydrodynamic Deep Drawing Assisted by Radial Pressure. *Iranian Journal of Science and Technology, Transactions of Mechanical Engineering*, 43(3), pp.487–494. Doi: 10.1007/s40997-018-0221-6



**Persian Abstract**

**چکیده**

صفحات دوقطبی نقش مهمی در پیل‌های سوختی از نظر وزن و هزینه ایفا می‌کنند. در این مقاله، ساخت صفحات دوقطبی با الگوی شیاری موازی از جنس تیتانیوم به‌صورت عددی و تجربی مورد بررسی قرارگرفته است. در این راستا، یک قالب مهرزنی با الگوی موازی برای انجام آزمایش‌ها ساخته شد. سپس فرآیند با استفاده از شبیه‌سازی اجزای محدود مدل شد. با مقایسه نتایج شبیه‌سازی و تجربی، مشخص شد که نتایج با هم مطابقت خوبی دارند و ازاین‌رو، صحت مدل اجزای محدود تأیید شد. برای ارزیابی شکل‌پذیری ورق تیتانیوم، مجموعه‌ای از آزمایش‌های المان محدود با استفاده از روش رویه پاسخ طراحی شد. لقی قالب، سرعت شکل‌دهی و ضریب اصطکاک به‌عنوان پارامترهای ورودی در نظر گرفته شدند و حداکثر کاهش ضخامت ورق به‌عنوان خروجی در نظر گرفته شد. نتایج نشان داد که ضریب اصطکاک کمتر باعث افزایش کاهش ضخامت و در نهایت پارگی در صفحات دوقطبی‌های تشکیل‌شده می‌شود. علاوه بر این، تغییر سرعت شکل‌دهی تأثیر قابل توجهی بر حداکثر کاهش ضخامت ندارد. در ادامه، یک سیستم استنتاج عصبی فازی تطبیقی برای پیش‌بینی خروجی حداکثر کاهش ضخامت با سه ورودی ذکرشده آموزش داده شد.